Investigation of intermittency in superfluid turbulence

Julien Salort, Benoît Chabaud, Emmanuel Lévêque, Philippe-Emmanuel Roche

Investigation of intermittency in superfluid turbulence

J. Salort[1], B. Chabaud[1], E. Lévêque[2] and P.-E. Roche[1]

[1]Institut Néel, CNRS/UJF, 25 rue des Martyrs, BP 166, F-38042 Grenoble cedex 9
[2]Laboratoire de Physique, ENS Lyon, CNRS/Université de Lyon, F-69364 Lyon

Abstract. This paper reports new experimental and simulation velocity data for superfluid steady turbulence above 1 K. We present values for the scaling exponent of the absolute value of velocity-increment structure functions. In both experiments and simulations, they evidence that intermittency occurs in superfluid flows in a quite comparable way to classical turbulence. In particular, the deviation from Kolmogorov 1941 keeps the same strength as we cross the superfluid transition. To the best of our knowledge, this is the first confirmation of the superfluid ^{4}He experimental results from Maurer & Tabeling (1998) and the first numerical evidence of intermittency in superfluid turbulence.

1. Introduction

Above $T_\lambda \approx 2.17\,\mathrm{K}$, liquid ^{4}He can be described by the Navier-Stokes equation. At T_λ, it undergoes a phase transition, the "superfluid" — or "Lambda" — transition. The new liquid phase below T_λ can be described as an intimate mixture of two components : the "normal" component which behaves like a classical Navier-Stokes fluid and the "superfluid" component with zero-viscosity and quantized vorticity. When this superfluid is strongly stirred, a tangle of quantum vortices is generated. The dynamics of this tangle is called "quantum turbulence". For an introduction to quantum turbulence, one may refer to Vinen & Niemela (2002).

The experimental investigation of turbulence in superfluid helium flows is a difficult problem if the academic standards of classical turbulence are to be met. It requires specifically designed probes and wind tunnels. Thus, until recently, very few local fluctuation measurements were available : there was only one famous velocity time series published 13 years ago, (Maurer & Tabeling, 1998). In the last couple of years, efforts have been made to produce new experiments, velocity and vorticity fluctuations have been measured in various geometries — grid flow, near wake flows and "chunk" flows. It revealed analogies (Salort *et al.*, 2010) but also differences (Roche *et al.*, 2007) between classical and superfluid "quantum" turbulence (Sergeev, 2011).

In this paper, we focus on the values of the scaling exponent of the absolute value of the longitudinal-velocity-increments in superfluid turbulence, obtained both experimentally in a new wind tunnel and numerically from recent high Reynolds number simulations (Salort *et al.*, 2011).

2. Wind tunnel and flow characteristics

The new cryogenic helium wind tunnel is similar to the one previously described in Roche *et al.* (2007) but much bigger and better optimized : the pipe is 90 cm long, 43 mm in diameter, filled with liquid helium hydrostatically pressurized by 1 m of helium to avoid cavitation at all temperatures (see figure 1). The propeller 3D-shape was optimized for this specific liquid helium wind tunnel and can achieve up to 130 g/s liquid helium mass flow. The probe is located 465 mm downstream a centered brass disk of 22 mm diameter. The flow seen by the probe is a far-wake turbulent signal with 4 % turbulence intensity. Above T_λ, the typical Reynolds number based on the Taylor microscale is $R_\lambda \approx 1500$.

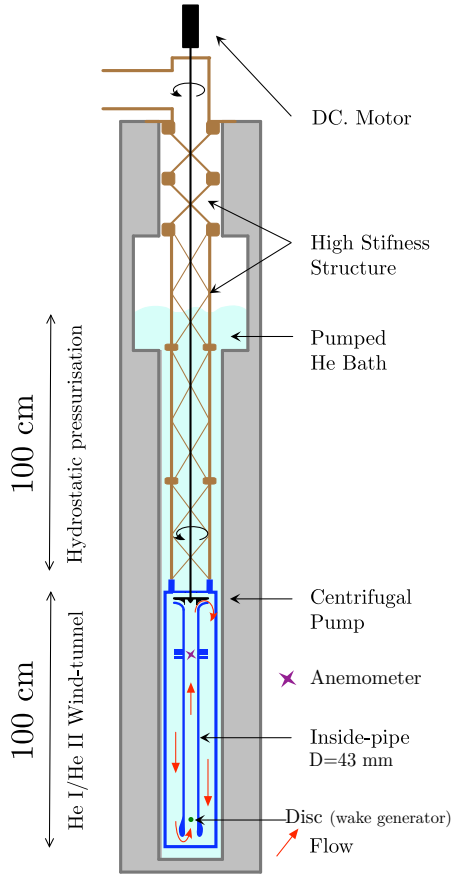

Figure 1. Sketch of the wind tunnel

The measurement is based on the recording of a velocity time series at one given location. The velocity sensor used in this wind tunnel is the probe ① described in Salort *et al.* (2010). It is inspired from the Pitot-tube design (stagnation pressure measurement), which is well fitted to flows with a few percent turbulence intensity. The velocity distribution is nearly Gaussian above and below the superfluid transition, as expected in classical turbulence at high Reynolds number (see inset of figure 2).

To compute statistics versus the flow scales, we use the instantaneous Taylor frozen turbulence hypothesis. When the turbulence intensity is a few percent or higher, using the average flow velocity to convert time in distances is spurious. We rather use the instantaneous velocity as described by Pinton & Labbé (1994). This leads to a space series $v(x)$ from which we can compute the power spectrum $E(k)$ using a Welch method. For reference, the spatial statistics

in Salort *et al.* (2010) were computed using a simpler Taylor hypothesis ($x = -\langle v \rangle t$) because the turbulence intensity was much smaller — of order 1 % in the grid flow.

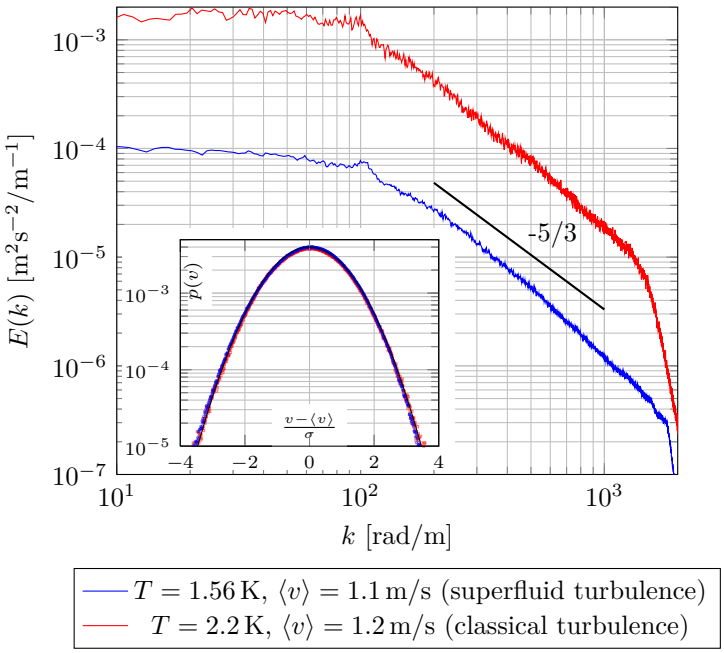

Figure 2. Experimental power spectrum of the velocity space series $v(x)$ computed using the instantaneous Taylor hypothesis. The low temperature time series is much longer (60 min) and therefore better averaged. Inset: Velocity histograms. Turbulence intensity in both cases : $\sigma / \langle v \rangle \approx 4\,\%$. Solid black line : Gaussian distribution.

Typical velocity power spectra $E(k)$ are given for recordings above and below the superfluid transition on figure 2. They are both fairly compatible with $k^{-5/3}$ Kolmogorov spectrum. The high-frequency cut-off comes from a numerical 4^{th}-order Butterworth filter applied before the time-to-space conversion and tuned to suppress the probe organ-pipe resonance. We computed velocity power spectra for various mean velocities at various temperatures above and below the superfluid transition and, as expected, we did not spot any significant difference above and below the superfluid transition.

From the velocity space series, we define the increment of the longitudinal velocity as,

$$\delta v(r) = v(x + r) - v(x) \tag{1}$$

For our experimental data, the mean values $\langle |\delta v(r)|^p \rangle$ are means over space x.

3. Numerical Simulation of superfluid turbulence

We investigate the turbulence of superfluid helium numerically at finite temperature using a continuous description : the "normal" component is modeled by the Navier-Stokes equation and the "superfluid" component by the Euler equation. A mutual coupling term $\vec{F}_{ns}$ is added to account for the mutual friction between the two components. It allows a consistent exchange of momentum between the normal component and the superfluid component. The model presented here has been described in Salort *et al.* (2011). The equations are summarized below,

$$\frac{D\vec{v}_n}{Dt} = -\frac{1}{\rho_n}\nabla p_n + \frac{\rho_s}{\rho}\vec{F}_{ns} + \frac{\mu}{\rho_n}\nabla^2\vec{v}_n + \vec{f}_n^{ext} \tag{2}$$

$$\frac{D\vec{v}_s}{Dt} = -\frac{1}{\rho_s}\nabla p_s - \frac{\rho_n}{\rho}\vec{F}_{ns} + \vec{f}_s^{ext} \tag{3}$$

where the indices n and s refer to the normal component and the superfluid, respectively, $\vec{f}_n^{ext}$ and $\vec{f}_s^{ext}$ are external forcing terms, μ is the dynamic viscosity. The mutual coupling term is approximated at first order,

$$\vec{F}_{ns} = -\frac{B}{2}\left|\vec{\omega}_s\right|\left(\vec{v}_n - \vec{v}_s\right) \tag{4}$$

where $\vec{\omega}_s = \nabla \times \vec{v}_s$ is the superfluid vorticity and $B \approx 2$ is the mutual friction coefficient.

This description is only valid for scales larger than a quantum scale δ corresponding to the typical inter-vortex spacing. We neglect the quantum effects that would occur at scale smaller than δ (Kelvin waves along vortices, for instance) because they are known to be evanescent at the finite temperature of interest here (say $T > 1\,\mathrm{K}$). Therefore we impose that the cut-off scale of the simulation corresponds to the quantum scale δ, estimated from the quantum of circulation κ around a single superfluid vortex and from the average vorticity,

$$\delta^2 = \frac{\kappa}{\sqrt{\left\langle \left|\vec{\omega}_s\right|^2 \right\rangle}} \tag{5}$$

In the following, we present new results from the post-processing of the simulated fields presented recently in Salort *et al.* (2011). As an illustration, the energy field of the normal component is shown on figure 3 for the high-temperature simulation. As a first step, we define a new field $\vec{v}_i$ that we call "Inertial velocity", defined as,

$$\left(\rho_n + \rho_s\right)\vec{v}_i = \rho_n\vec{v}_n + \rho_s\vec{v}_s \tag{6}$$

This quantity $\vec{v}_i$ is close to what actual stagnation pressure probes measure in experiments. Indeed, such probes are sensitive to the momentum on their tips, and therefore to the local momentum $(\rho_n + \rho_s)\vec{v}_i$. At high temperature where $\rho_s/\rho_n \ll 1$ — for example at $T \approx 2.1565\,\mathrm{K}$, $\rho_s/\rho_n = 0.1$ — we get $\vec{v}_i \approx \vec{v}_n$. At low temperature where $\rho_s/\rho_n \gg 1$ — for example at $T \approx 1.15\,\mathrm{K}$, $\rho_s/\rho_n = 40$ — we get $\vec{v}_i \approx \vec{v}_s$.

We compute the longitudinal inertial velocity increments along each direction, $\delta_x(r) = v_{i,x}(x+r) - v_{i_x}(x)$, $\delta_y(r) = v_{i,y}(y+r) - v_{i,y}(y)$, $\delta_z(r) = v_{i,z}(z+r) - v_{i,z}(z)$ and we average the structure function of interest over the three directions, eg.

$$\langle|\delta v(r)|^p\rangle = \frac{1}{3}\left(\langle|\delta_x(r)|^p\rangle + \langle|\delta_y(r)|^p\rangle + \langle|\delta_z(r)|^p\rangle\right) \tag{7}$$

4. Exponent of the structure functions

For r in the inertial range, the scaling exponent $\zeta(p)$ of the absolute value of the velocity-increment structure function is defined as,

$$SF(p) = \langle|\delta v(r)|^p\rangle \sim r^{\zeta(p)} \tag{8}$$

Following Benzi *et al.* (1993), extended self-similarity is used to compute $\zeta(p)$: $SF(p)$ is plotted against $SF(3)$. It follows

$$SF(p) = SF(3)^{\zeta(p)/\zeta(3)} \tag{9}$$

Then, in practice, we take $\zeta(3) = 1$ and $\zeta(p)$ is determined from the plateau of the logarithmic derivative,

$$\zeta(p) = \frac{\mathrm{d}\log SF(p)}{\mathrm{d}\log SF(3)} \tag{10}$$

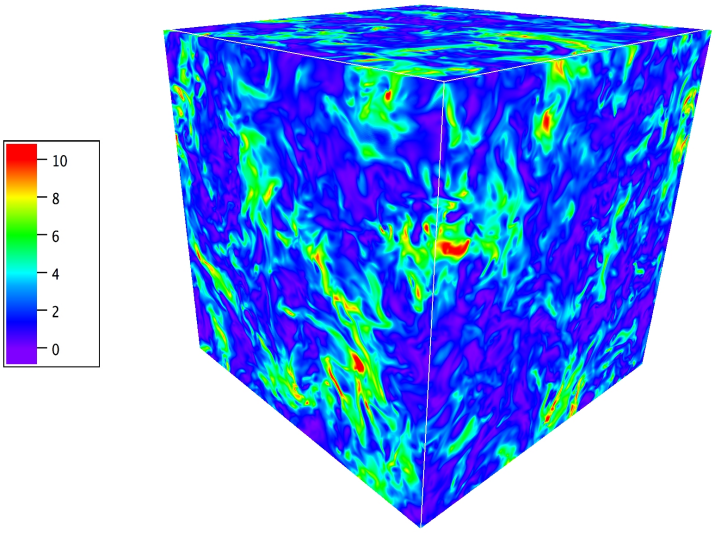

Figure 3. Kinetic energy of the normal component normalized by its space-averaged kinetic energy at $T \approx 2.1565\,\mathrm{K}$ ($\rho_s/\rho_n = 0.1$). The periodic box size is 512^3.

The fluctuations of the logarithmic derivative are taken as an estimate of the error on $\zeta(p)$.

As is shown on figure 4, the experimental fluctuations above the superfluid transition ($T = 2.2\,\mathrm{K}$) lead to exponents $\zeta(p)$ that deviate from the Kolmogorov 1941 $p/3$ prediction at high p, which accounts for intermittency in this flow. The results obtained in the exact same wind tunnel, with nearly the same mean velocity both below and above the superfluid transition (resp. at $T = 1.56\,\mathrm{K}$, $\rho_s/\rho_n \approx 5.78$ and $T = 2.2\,\mathrm{K}$) match within error bars. This suggests that intermittency in this type of flow does not change when the temperature crosses the superfluid transition.

Numerical simulations over a wide range of temperature in the superfluid domain all lead to exponents $\zeta(p)$ that collapse together, and we note that they overlap with the intermittency model from She & Leveque (1994).

Both experimental and numerical results suggest that intermittency can occur in superfluid flows in a quite comparable way to classical turbulence. However, we shall point out that in both cases, the small scale fluctuations are filtered out. This comes either from the high-frequency cut-off of the anemometer or from the numerical coarse-graining from which the Euler equation is derived. Therefore, the results might have differed if the velocity singularities associated with the quantum vortices had not been filtered out by the probe and the numerical model.

5. Conclusions

The pioneering measurement of Maurer & Tabeling (1998) in superfluid helium, also plotted on figure 4, suggested that intermittency in superfluid turbulence was similar to intermittency in classical turbulence. Our results confirm this conclusion and allow direct comparison of $\zeta(p)$ for classical and superfluid conditions measured with the same setup and for the same mean velocity. This experimental result is completed by the first numerical simulations that lead to intermittency evaluation in a continuous model of superfluid turbulence. These simulations were performed over a wide range of temperatures in the superfluid domain. The evaluated intermittency exhibited no significant difference when the ratio of the superfluid component is

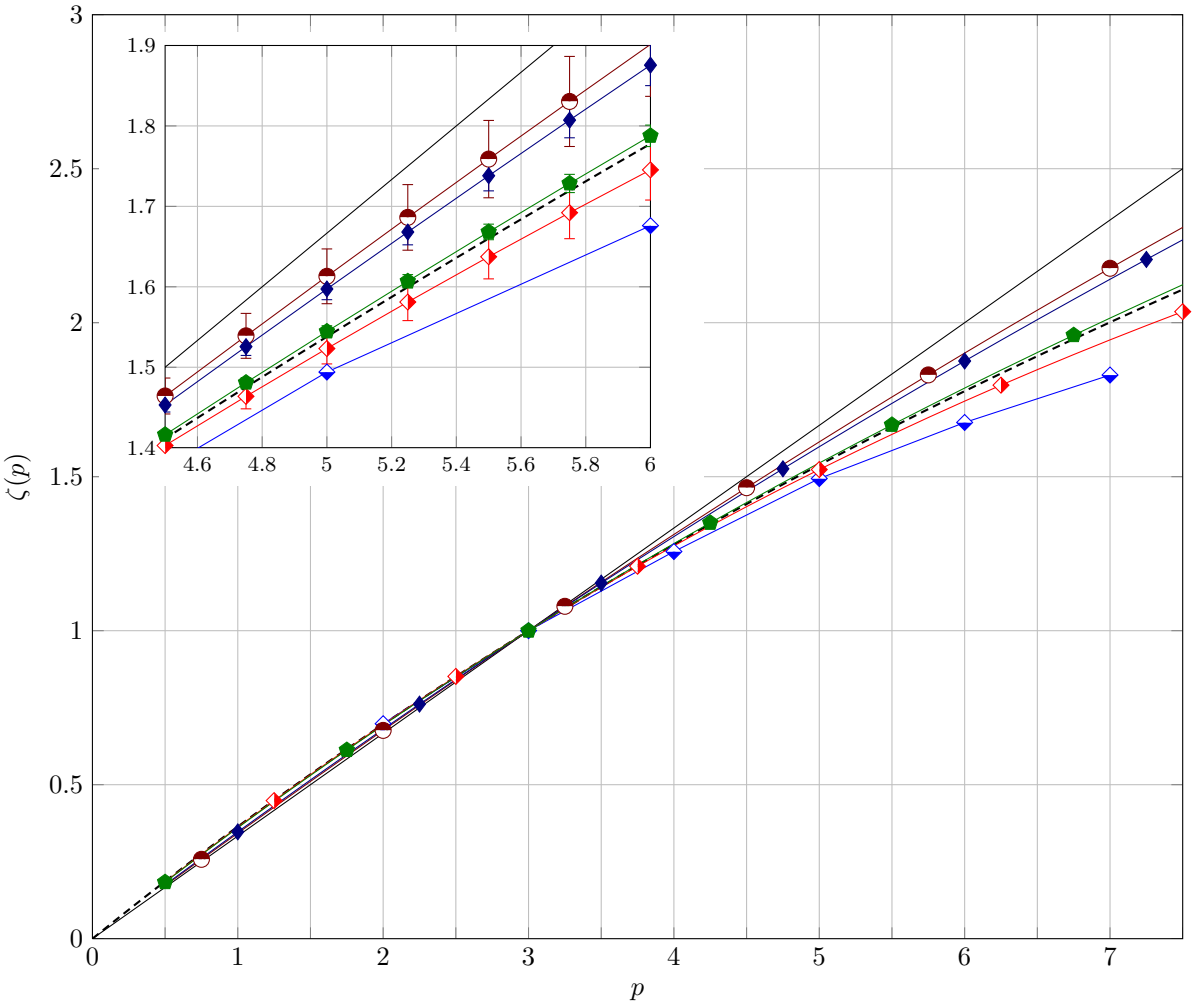

T < T$_\lambda$

- Present experiment @ 1.56 K
- Present simulation (512^3) @ 2.1565 K
- Present simulation (512^3) @ 1.15 K
- Von Kármán @ 1.4 K (Maurer and Tabeling 1998)

T > T$_\lambda$

- Present experiment @ 2.2 K ($R_\lambda \approx 1500$)
- $p/3$ (Kolmogorov)
- $p/9 + 2\left[1 - \left(\frac{2}{3}\right)^{p/3}\right]$ (She-Leveque)

Figure 4. Scaling exponent of the absolute value of the longitudinal-velocity-increment $\zeta(p)$. Inset: Zoom for $4.5 < p < 6$ with error bars. For readability, the main figure shows only one every five markers.

increased from $\rho_s/\rho_n = 0.1$ to $\rho_s/\rho_n = 40$.

The present experiment and the experimental values from Maurer & Tabeling (1998) show slight discrepancies. We suspect that they may come from geometrical differences in the flows but this would require further investigation.

Acknowledgments

This work benefited from the financial support of the ANR (grants "SHREK" ANR-09-BLAN-0094 and "TSF" ANR-05-BLAN-0316) and from the local computing facilities from PSMN at ENS Lyon and HPC resources from GENCI-CINES (grants 2010-026380 and 2011-026380). We are grateful to Pierre Chanthib, Anne Gerardin, Christophe Guttin and for their help and support. We are grateful to Étienne Ghiringhelli, Pierre-Luc Delafin, Jacques Depont and Jean-Louis Kueny for their work on the design of the cryogenic centrifugal pump.

References

Benzi, R., Ciliberto, S., Tripiccione, R., Baudet, C., Massaioli, F. & Succi, S. 1993 Extended self-similarity in turbulent flows. *Phys. Rev. E* **48** (1), R29–R32.

Maurer, J. & Tabeling, P. 1998 Local investigation of superfluid turbulence. *EPL* **43** (1), 29–34.

Pinton, J.-F. & Labbé, R. 1994 Correction to the taylor hypothesis in swirling flows. *J. Phys. II* **4**, 1461–1468.

Roche, P.-E., Diribarne, P., Didelot, T., Français, O., Rousseau, L. & Willaime, H. 2007 Vortex density spectrum of quantum turbulence. *EPL* **77**, 66002.

Salort, J., Diribarne, P., Rousset, B., Gagne, Y., Dubrulle, B., Didelot, T., Chabaud, B., Gauthier, F., Castaing, B. & Roche, P.-E. 2010 Turbulent velocity spectra in superfluid flows. *Phys. fluids* **22**, 125102.

Salort, J., Roche, P.-E. & Lévêque, E. 2011 Mesoscale equipartition of kinetic energy in quantum turbulence. *EPL* **94**, 24001.

Sergeev, Yuri 2011 Quantum turbulence: Energy dissipation in extreme cold. *Nature Physics* **7**, 451–452.

She, Zhen-Su & Leveque, Emmanuel 1994 Universal scaling laws in fully developed turbulence. *Phys. Rev. Lett.* **72** (3), 336.

Vinen, W. F. & Niemela, J. J. 2002 Quantum turbulence. *J. Low Temp. Phys.* **128** (5/6), 167.